J Mol Model (2005) 11: 186–193
DOI 10.1007/s00894-004-0233-6

ORIGINAL PAPER

Wensheng Cai · Yanmin Yu · Xueguang Shao

Chiral recognition of aromatic compounds by β-cyclodextrin based on bimodal complexation

Received: 7 June 2004 / Accepted: 22 November 2004 / Published online: 18 May 2005

Abstract The chiral recognition of the selected aromatic chiral compounds by native β-cyclodextrin (β-CD) based on bimodal complexation was studied using a flexible docking algorithm FDOCK. A quantitative empirical free energy relationship model was employed to predict the complex stability constants and the preferred binding modes. The results showed that the calculated complex stability constants are in good agreement with the experimental data. Furthermore, the main force responsible for host-guest complexation is the van der Waals force and the chiral molecules are completely included into the β-CD cavity. The chiral recognition for the selected aromatic chiral compounds is the result of the van der Waals force counterbalancing with the other effects, such as the electrostatic interaction and the hydrophobic effect.

Keywords Chiral recognition · Aromatic chiral compounds · β-cyclodextrin · Bimodal complexation · Flexible docking algorithm

Introduction

Chiral recognition, as an aspect of molecular recognition, has been a subject of great interest because the majority of bioorganic molecules are chiral and the behavior of enantiomers in a chiral environment is different. The most important property of cyclodextrins (CDs) is their capability of forming complexes with the appropriate guest molecules [1]. Furthermore, the inherent chirality of the cyclodextrin molecules allows them to form a diastereomeric pair of inclusion complexes with each enantiomer of a racemate. The natural chiral cyclodextrins and their derivatives have been used extensively as models for investigating chiral recognition by various experiment techniques [2–8]. Computer simulations are frequently used to rationally explain the experimental findings concerning inclusion and recognition [9–14]. In our initial studies, the chiral recognition of α-cyclodextrin in vacuum was studied, in which the host and the guest were considered as rigid bodies [15]. In our recent work, a docking algorithm FDOCK, [16] which considers the flexibility of host and guest molecules, was used to study the chiral recognition of native β-cyclodextrin (β-CD) in aqueous solution based on bimodal complexation.

Our efforts in this paper are devoted to the chiral recognition properties of β-CD using a docking approach. The chiral recognition of nine pairs of aromatic chiral compounds (18 guest molecules) by native β-CD in aqueous solution was studied using FDOCK on the basis of bimodal complexation. A quantitative nonlinear empirical free energy relationship model, which uses each component energy term of the lowest energy complex structure, was employed to calculate the complex stability constants. The results show that the calculated stability constants are in agreement with the experimental data. By analyzing each energy term and the average interaction energy difference between the enantiomers, the main driving force responsible for complexation and the dominant factor in chiral recognition are elucidated.

Theory and method

Molecular model

The original structure of native β-CD was taken from the literature. [17] The initial structures of chiral compounds were built by Insight II software. The

W. Cai (✉) · Y. Yu · X. Shao
Department of Chemistry,
University of Science and Technology of China,
Hefei, Anhui, 230026, People's Republic of China
E-mail: wscai@ustc.edu.cn
Tel.: +86-551-3606160
Fax: +86-551-3601592

structural formulas of the selected chiral molecules are illustrated in Fig. 1, and the corresponding chiral atoms are labeled with '*'. The abbreviations of the chiral molecules are listed in Table 1. All the initial structures were energy-minimized using the conjugate gradient method with the CFF91 force field in the Discover module of Insight II. In this study, two main binding modes, depending on which group of the guest is firstly included into the cavity from the wider rim of CD, were taken into account. The sketches of two main binding modes (model A and model B) are shown in Fig. 2. In which, β-CD was oriented to have almost all the glycosidic oxygen atoms in the XY-plane, and the origin of the coordinate system was placed at the geometry center of β-CD. The Z-axis is perpendicular to the XY-plane through the origin and pointing to the primary side of β-CD. The position of the chiral molecule in the β-CD cavity is defined by the coordinate of its geometry center. Therefore, the Z-coordinate represents the geometry center position of the guest molecule relative to β-CD, reflecting the inclusion depth of the guest molecule in the cavity. The two binding modes were calculated in two independent runs of FDOCK by rotating the orientation of the guest molecule to model A or B as the initial input structure and keeping the orientation during moving.

Flexible docking

All the calculations were performed using the flexible docking algorithm FDOCK, which is a combination of the global optimization algorithm FAEA [18] with a local optimization algorithm L-BFGS. [19] In the FDOCK, the consistent force field (CFF91) [20] is adopted to evaluate the energy involved in the complexation process, and an implicit solvent model [21] is applied to calculate the solvation energy of the complexation.

In rigid docking, the parameters to be optimized are the relative position (T_x, T_y, T_z) and the relative orientation (θ, ϕ, ψ) of the guest molecule in the cavity of CD. It is suitable for a less flexible system, [15] however, in flexible docking, the internal coordinates of each molecule also need to be optimized since all the interactive molecules are flexible. In this paper, the host (β-CD) was firstly fixed at the original point as in Fig. 2. The guest (chiral compound) was located at the wide side of the cavity and 5 Å away from the host, then, it was moved across the cavity along the Z-axis step by step to the narrow side. In each step, the relative position (T_x, T_y, T_z) and the relative orientation (θ, ϕ, ψ) of the guest molecule in the cavity of CD were optimized by FAEA, and the coordinates of the host and guest molecules each with a given relative position were optimized with L-

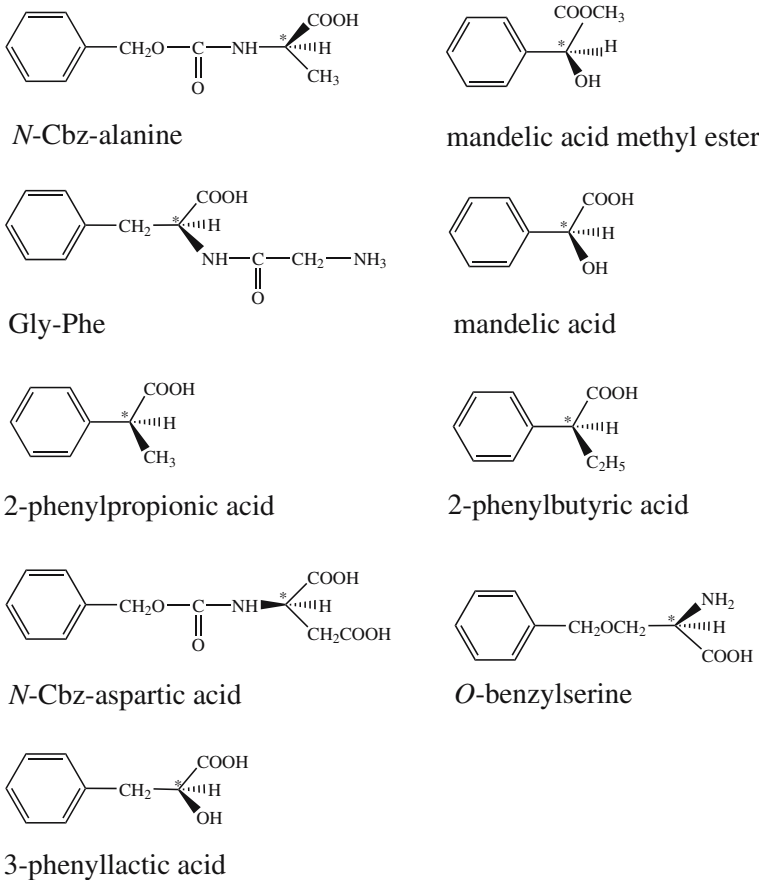

Fig. 1 The structures of guest molecules

Table 1 Chiral guests and corresponding abbreviations

No.	Chiral guest molecules (charge)	Abbreviation[a]
1	*N*-Cbz-D-alanine (−1)	D_Cbz_alanine
2	*N*-Cbz-L-alanine (−1)	L_Cbz_alanine
3	*N*-glycine-D-phenylalanine (zwitterion)	D_gly_phe
4	*N*-glycine-L-phenylalanine (zwitterion)	L_gly_phe
5	(*R*)-mandelic acid methyl ester (0)	(*R*)_m_mandelic
6	(*S*)-mandelic acid methyl ester (0)	(*S*)_m_mandelic
7	(*R*)-mandelic acid (−1)	(*R*)_mandelic
8	(*S*)-mandelic acid (−1)	(*S*)_mandelic
9	(*R*)-2-phenylpropionic acid (−1)	(*R*)_phenylpropionic
10	(*S*)-2-phenylpropionic acid (−1)	(*S*)_phenylpropionic
11	*N*-Cbz-D-aspartic acid (−2)	D_Cbz_aspartic
12	*N*-Cbz-L-aspartic acid (−2)	L_Cbz_aspartic
13	*O*-benzyl-D-serine (zwitterion)	D_benzyl_serine
14	*O*-benzyl-L-serine (zwitterion)	L_benzyl_serine
15	(*R*)-2-phenylbutyric acid (−1)	(*R*)_phenylbutyric
16	(*S*)-2-phenylbutyric acid (−1)	(*S*)_phenylbutyric
17	(*R*)-3-phenyllactic acid (−1)	(*R*)_phenyllactic
18	(*S*)-3-phenyllactic acid (−1)	(*S*)_phenyllactic

[a]The abbreviations of chiral guests will be used in the following tables

BFGS. Furthermore, a random local search procedure was also used to optimize both the relative position and orientation of the guest molecule in the cavity, as well as the atomic coordinates of each molecule. The optimized structure of each step was saved to a trajectory file for further analysis.

Binding free energy function

The CFF91 force field was used to deal with the interaction energies and intramolecular energies of the host and guest. The distance-dependent dielectric constant $\varepsilon = 4r_{ij}$ is used in the calculations. The empirical free energy of binding is given by

$$\Delta G_{\text{total}} = E_{\text{inter}} + \Delta E_{\text{intra}} + \Delta G_{\text{sol}} \tag{1}$$

in which, the interaction energy E_{inter} consists of the van der Waals term E_{vdw} and the electrostatic term E_{elec} between the host and guest molecules. ΔE_{intra} is the energy involved in the deformation of the host and the guest, including bond stretching, angle bending, torsion energy, out of plane bending and all the cross terms, as in Eq. 2.

$$\begin{aligned}\Delta E_{\text{intra}} =& \Delta E_{\text{vdw}} + \Delta E_{\text{elec}} + \Delta E_{\text{bond}} + \Delta E_{\text{angle}} + \Delta E_{\text{tor}} \\ &+ \Delta E_{\text{out\_of\_plane}} + \Delta E_{\text{bond\_bond}} \\ &+ \Delta E_{\text{angle\_angle}} + \Delta E_{\text{bond\_angle}} \\ &+ \Delta E_{\text{bond\_dihedral}} + \Delta E_{\text{angle\_dihedral}} \\ &+ \Delta E_{\text{angle\_angle\_dihedral}} + \Delta E_{\text{bond\_bond\_1\_3}}\end{aligned} \tag{2}$$

Also, in Eq. 1, ΔG_{sol} is the solvation free energy. An implicit solvent model [21] based on a very efficient analytical evaluation of the solvent accessible surface area (SASA) [22] was employed to calculate the solvation energy of the complexation. The solvation free energy is calculated by

$$\begin{aligned}\Delta G_{\text{sol}} &= G_{\text{sol}}^{\text{complex}} - G_{\text{sol}}^{\text{free - host}} - G_{\text{sol}}^{\text{free - guest}} \\ &= \sum_{i=1}^{N_h+N_g} \sigma_i \Delta A_i\end{aligned} \tag{3}$$

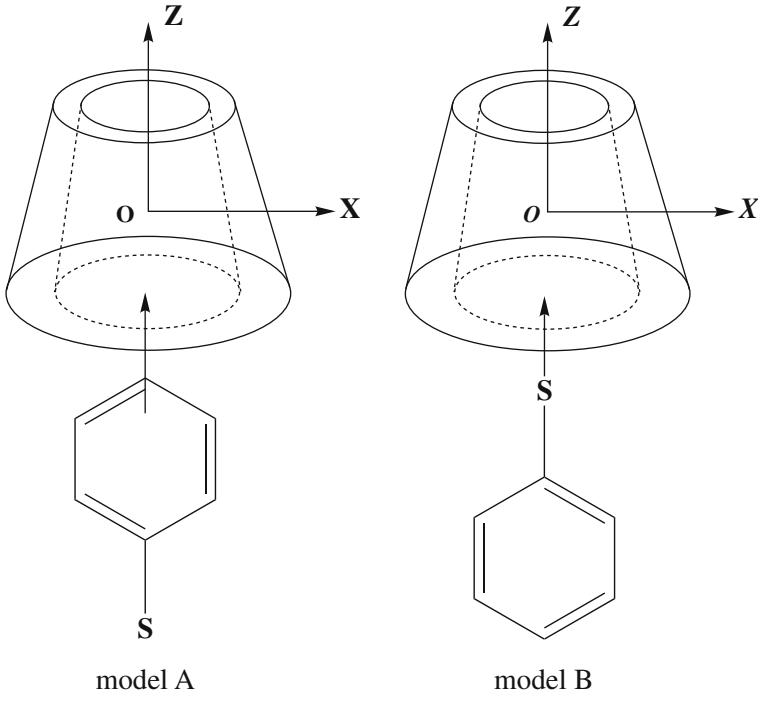

Fig. 2 The two possible complexation models of the chiral guest with β-CD. 'S' represents the substituent on the benzene ring

where σ_i is the solvation parameters of each atom type, and ΔA_i is the difference between the solvent accessible surface area of the ith atom in the complex and the surface area of the same atom in the isolated state. In our study, the solvation effect of all the atoms of the host and guest were calculated.

Stability of bimodal complexes

A quantitative nonlinear empirical free energy relationship model based on each energy term of the lowest energy structure was employed to calculate the stability constants. In this model, two possible binding orientations (model A and model B) are taken into account, [23] where,

$$\begin{aligned}\ln K &= \ln(K_{\mathrm{A}} + K_{\mathrm{B}}) \\ K_{\mathrm{A}} &= \exp(-\frac{1}{RT}(a_0 + a_1 E^{\mathrm{A}}_{\mathrm{vdw}} + a_2 E^{\mathrm{A}}_{\mathrm{elec}} \\ &\quad + a_3 \Delta E^{\mathrm{A}}_{\mathrm{intra}} + a_4 \Delta G^{\mathrm{A}}_{\mathrm{sol}})) \\ K_{\mathrm{B}} &= \exp(-\frac{1}{RT}(a_0 + a_1 E^{\mathrm{B}}_{\mathrm{vdw}} + a_2 E^{\mathrm{B}}_{\mathrm{elec}} + a_3 \Delta E^{\mathrm{B}}_{\mathrm{intra}} \\ &\quad + a_4 \Delta G^{\mathrm{B})}_{\mathrm{sol}}) \end{aligned} \tag{4}$$

in which, E_{vdw}, E_{elec}, $\Delta E_{\mathrm{intra}}$ and ΔG_{sol} are the component energy terms of the lowest energy complex structure. The coefficients in the above nonlinear equation were estimated by minimizing the error function:

$$\mathrm{err} = \frac{1}{N}\sum_{i=1}^{N}[\ln K_i^{\mathrm{pred}} - \ln K_i^{\mathrm{obs}}]^2 \tag{5}$$

where, $\ln k_i^{\mathrm{obs}}$ are given by experimental methods. [2, 3] In our study, the error function was optimized using the L-BFGS algorithm. [19]

Results and discussion

Forces responsible for complexation and the binding site of guest in the β-CD cavity

The basic mechanism of chiral recognition by CDs is the inclusion interactions between CDs and enantiomers. How and where the guest binds enantioselectively to the CD cavity is a very important problem. In order to answer this question, β-CD was firstly fixed at the original point and the guest was introduced into the cavity from the secondary rim of β-CD in two ways (model A and model B in Fig. 2). At first, the guest was located at the wide side of the CD cavity and 5 Å away from β-CD by setting $Z = -5$Å. The Z-coordinate represents the geometry center position of the guest molecule relative to β-CD, and reflects the inclusion depth of the guest molecule in the cavity. Then, the guest was moved in the cavity along Z-axis from −5 Å to 5 Å in steps of 0.1 Å, and the initial complex structure can be obtained for each step. The initial complex structure was subsequently optimized using FDOCK to perform the docking process between the guest and β-CD. The optimized structure and the corresponding energy values of this step were saved to the trajectory file. Finally, the lowest energy structure was chosen from the optimized structures with different Z-coordinates and considered as the most stable complex structure of β-CD with the guest. The two binding modes were calculated in two independent runs of FDOCK by rotating the orientation of the guest molecule to model A or B as the initial input structure, and keeping the orientation during moving. For each binding mode, the component energy terms and the corresponding Z-coordinates of the most stable complex structures of β-CD with the chiral compounds are listed in Table 2. This allows us to identify where the guest prefers to bind to the β-CD cavity.

From Table 2, it is clear that no large energy difference was found between the complexes for the two orientations of each enantiomer. Therefore, we roughly considered that both the complexes of the two orientations are stable, and it is necessary to calculate bimodal complexation in chiral recognition. Analyzing each component energy term, it is apparent that the magnitude of van der Waals force is much larger than that of any other energy terms. Therefore, the van der Waals force is the main driving force responsible for the complexation. In addition, it can also be seen from Table 2 that $Z \in [-1.5$ Å, 1.5 Å], which reveals that the preferential binding site for the selected aromatic chiral compound is the interior of the β-CD cavity and the chiral compounds are completely included into the β-CD cavity.

Prediction of the stability constants and the favorable orientations of complexation

From the above docking procedure, the lowest energy structure for each binding mode was finally chosen from the 100 optimized structures and considered as the most stable complex structure of β-CD with the chiral molecule. The corresponding energies of the most stable complex structures were used to predict the stability constants of the two modes.

A quantitative model based on each component energy term listed in Table 2 was employed to predict the complex stability constants. The calculated stability constants $\ln K_{\mathrm{pred}}$ were listed in Table 3 together with the experimental stability constants $\ln K_{\mathrm{obs}}$. Comparing $\ln K_{\mathrm{pred}}$ with $\ln K_{\mathrm{obs}}$, it is clear that the calculated stability constants are in agreement with those determined by the experimental method, and the rank of $\ln K_{\mathrm{pred}}$ value is coincident with that of $\ln K_{\mathrm{obs}}$ for each pair of enantiomers.

In Table 3, $\ln K_{\mathrm{A}}$ and $\ln K_{\mathrm{B}}$ reflect the stability of the two possible orientation complexes, respectively. The larger $\ln K$ value corresponds to the more stable complex model. From this quantitative information, the favor-

Table 2 The component energies obtained by FDOCK for 18 guest molecules with β-CD

[a]The energy unit is kcal mol^{-1}, and $\Delta G_{total} = E_{vdw} + E_{elec} + \Delta G_{sol} + \Delta E_{intra}$
The unit of Z values is Å

Guest	Model	ΔG_{total}	E_{vdw}	E_{elec}	ΔG_{sol}	ΔE_{intra}	Z
D_Cbz_alanine	A	−29.910	−29.547	−2.206	4.473	−2.629	−1.316
	B	−30.189	−28.184	−2.516	3.050	−2.538	0.727
L_Cbz_alanine	A	−29.127	−28.073	−1.309	3.376	−3.121	−1.163
	B	−30.809	−29.234	−3.213	3.852	−2.214	0.889
D_gly_phe	A	−27.021	−29.412	−0.761	4.483	−1.331	−0.529
	B	−26.902	−28.819	−1.215	4.337	−1.205	1.268
L_gly_phe	A	−27.541	−29.966	−1.400	4.450	−0.626	−0.853
	B	−26.576	−31.191	0.370	4.790	−0.547	0.657
(*R*)_m_mandelic	A	−30.987	−24.749	−0.028	2.540	−8.750	0.335
	B	−30.328	−24.924	−0.072	2.985	−8.317	−1.081
(*S*)_m_mandelic	A	−31.074	−25.391	−0.234	2.658	−8.107	−0.346
	B	−30.581	−25.683	−0.090	2.998	−7.805	−1.021
(*R*)_mandelic	A	−21.273	−23.701	−1.401	3.408	0.421	0.524
	B	−21.173	−21.330	−2.423	2.863	−0.283	1.097
(*S*)_mandelic	A	−21.277	−23.793	−0.553	3.530	−0.462	0.700
	B	−20.850	−22.873	−1.851	4.068	−0.193	−1.282
(*R*)_phenylpropionic	A	−21.535	−23.935	−1.264	2.411	1.253	0.078
	B	−21.559	−23.614	−1.202	2.434	0.822	0.388
(*S*)_phenylpropionic	A	−22.405	−24.430	−0.508	2.384	0.149	0.297
	B	−21.208	−22.771	−1.332	2.302	0.594	−0.126
D_Cbz_aspartic	A	−32.111	−33.894	−3.452	6.254	−1.001	0.271
	B	−32.980	−32.577	−4.397	5.668	−1.674	0.627
L_Cbz_aspartic	A	−32.254	−34.950	−2.427	6.433	−1.310	1.079
	B	−33.821	−34.842	−2.642	6.227	−2.564	0.003
D_benzyl_serine	A	−23.463	−28.585	−1.023	4.014	2.130	−0.996
	B	−23.071	−27.113	−0.847	3.565	1.325	0.766
L_benzyl_serine	A	−22.713	−28.302	−0.546	3.670	2.466	−0.589
	B	−21.862	−23.853	−0.611	2.775	−0.174	1.119
(*R*)_phenylbutyric	A	−23.670	−25.536	−1.182	2.190	0.858	−0.359
	B	−23.701	−25.456	−1.173	2.270	0.659	−0.087
(*S*)_phenylbutyric	A	−24.312	−26.381	−0.523	2.275	0.318	0.463
	B	−23.405	−25.331	−1.209	2.270	0.865	−0.113
(*R*)_phenyllactic	A	−24.745	−25.615	−1.013	3.466	−1.582	0.253
	B	−25.208	−24.647	−1.616	3.218	−2.163	0.042
(*S*)_phenyllactic	A	−24.348	−25.118	−0.558	3.312	−1.984	0.157
	B	−24.620	−24.409	−1.623	3.304	−1.892	−0.361

Table 3 Predicted and experimental complex stability constants for the inclusion complexation of nine pairs of enantiomers with β-CD

Guest	ln K_A[a]	ln K_B[a]	ln K_{pred}[a]	ln K_{obs}[b]
D_Cbz_alanine	3.625	4.513	4.857	5.004
L_Cbz_alanine	4.051	4.198	4.820	4.990
D_gly_phe	3.321	3.291	3.999	3.850
L_gly_phe	3.590	3.495	4.237	3.989
(*R*)_m_mandelic	3.801	3.423	4.323	4.205
(*S*)_m_mandelic	3.910	3.660	4.486	4.277
(*R*)_mandelic	2.247	2.066	2.854	2.398
(*S*)_mandelic	2.113	1.409	2.515	2.197
(*R*)_phenylpropionic	3.214	3.093	3.849	3.526
(*S*)_phenylpropionic	3.391	2.941	3.884	3.584
D_Cbz_aspartic	3.486	3.800	4.348	4.258
L_Cbz_aspartic	3.679	3.931	4.506	4.308
D_benzyl_serine	3.303	3.219	3.955	4.263
L_benzyl_serine	3.450	2.841	3.884	4.234
(*R*)_phenylbutyric	4.017	3.922	4.664	4.543
(*S*)_phenylbutyric	4.194	3.870	4.738	4.554
(*R*)_phenyllactic	2.952	2.941	3.640	4.477
(*S*)_phenyllactic	2.886	2.759	3.518	4.419

[a]ln K_A (for model A), ln K_B (for model B), and ln K_{pred} were calculated by Eq. 4, where $a_0 = 1.915$, $a_1 = 0.214$, $a_2 = 0.034$, $a_3 = 0.069$, $a_4 = 0.563$
[b]ln K_{obs} was published in References [2, 3]

able orientation can be suggested. The histogram of calculated complex binding constants for the two orientations of each pair of enantiomers is shown in Fig. 3. It is obvious that model B is more stable for the complexes of D/L_Cbz_alanine and D/L_Cbz_aspartic, whereas model A is more stable for the complexes of the other chiral molecules. It is possible that the introduction of Cbz group converts the hydrophobicity order of the guest. Accordingly, the preferred orientation is changed [3].

Forces responsible for chiral recognition

The energy difference between the enantiomeric complexes was frequently used as a measure of chiral recognition. While the van der Waals force is mostly responsible for holding the host-guest complex together, there is no basis to predict that it is also responsible for chiral recognition. To determine which is the main factor in chiral recognition, the average interaction energy of the two orientations was investigated. The differences in average interaction energy between the enantiomeric complexes are summarized in Table 4, and the largest

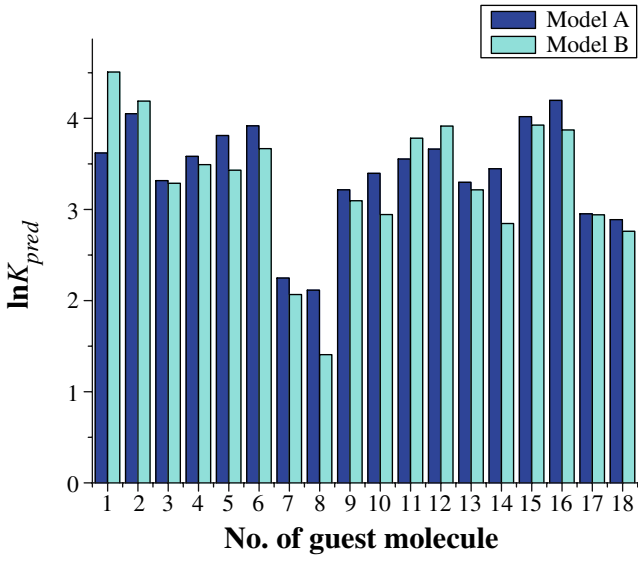

Fig. 3 The histogram of the calculated binding constants for the two complexation models

difference values for each pair of enantiomeric complexes are given in bold type.

From Table 4, it is clear that the difference of the van der Waals force is larger in magnitude than that of any other energy terms for the complexes of each pair of enantiomers except for (*R*/*S*)_phenylpropionic. For (*R*/*S*)_phenylpropionic complexes, the largest energy difference exists in the electrostatic energy term. Hence, the domain factor in chiral recognition of (*R*/*S*)_phenylpropionic enantiomers is the difference of electrostatic interaction. While for the other enantiomeric pairs, the main forces responsible for chiral recognition are the van der Waals forces.

For D/L_Cbz_aspartic with two negative charges, although the largest energy difference exists in the van der Waals force, the electrostatic interaction even the hydrophobic effect also plays an important role in chiral recognition. Furthermore, the differences of the electrostatic interaction and the hydrophobic effect, which have the contrary sign with that of the van der Waals interaction, can compensate the difference of van der Waals force and hence weaken its ability to drive chiral recognition. Therefore, the chiral recognition of D/L_Cbz_aspartic enantiomers is governed by the counterbalance between the van der Waals force and the other effects, such as the electrostatic interaction and the hydrophobic effect.

Table 4 The differences in average interaction energy of the two-binding modes for each pair of enantiomers with β-CD

No	Guest	ΔE_{vdw} [a]	ΔE_{elec}	$\Delta\Delta G_{sol}$
1	Cbz_alanine	**−0.212**	−0.100	0.148
2	Gly_phe	**1.463**	−0.473	−0.210
3	M_mandelic	**0.701**	0.112	−0.066
4	Mandelic	**0.818**	−0.710	−0.664
5	Phenylpropionic	−0.174	**−0.313**	0.080
6	Cbz_aspartic	**1.661**	−1.390	−0.369
7	Benzyl_serine	**−1.772**	−0.357	0.567
8	Phenylbutyric	**0.360**	−0.312	−0.043
9	Phenyllactic	**−0.368**	−0.224	0.034

[a]The energy unit is kcal mol^{-1}.
[b]For chiral aromatic amino acid derivatives $\Delta E_{vdw} = E_{vdw}$(D) − E_{vdw}(L), ΔE_{elec}, $\Delta\Delta G_{sol}$ have the same definition
For chiral benzene derivatives $\Delta E_{vdw} = E_{vdw}(R) - E_{vdw}(S)$, ΔE_{elec}, $\Delta\Delta G_{sol}$ have the same definition

For phenylbutyric and phenyllactic, it can be seen from Table 4 that the energy difference magnitudes of the two enantiomeric pairs are very close. However, an appreciable chiral recognition for phenyllactic was observed, while phenylbutyric do not undergo enantioselective binding with β-CD [3]. To elucidate this problem, the cooperativity or the compensation of several interactions responsible for the chiral recognition was investigated. For phenylbutyric, the two main factors in chiral recognition ($\Delta E_{vdw} = 0.360$ kcal mol^{-1}, $\Delta E_{elec} = -0.312$ kcal mol^{-1}) are of the contrary signs. The elec-

Fig. 4 The favorable structures for the inclusion complexes of D_benzyl_serine with β-CD. β-CD and D_benzyl_serine are drawn in line and stick, respectively. **a** View in the plane normal to the *Z*-axis. **b** View in the *ZX*-plane

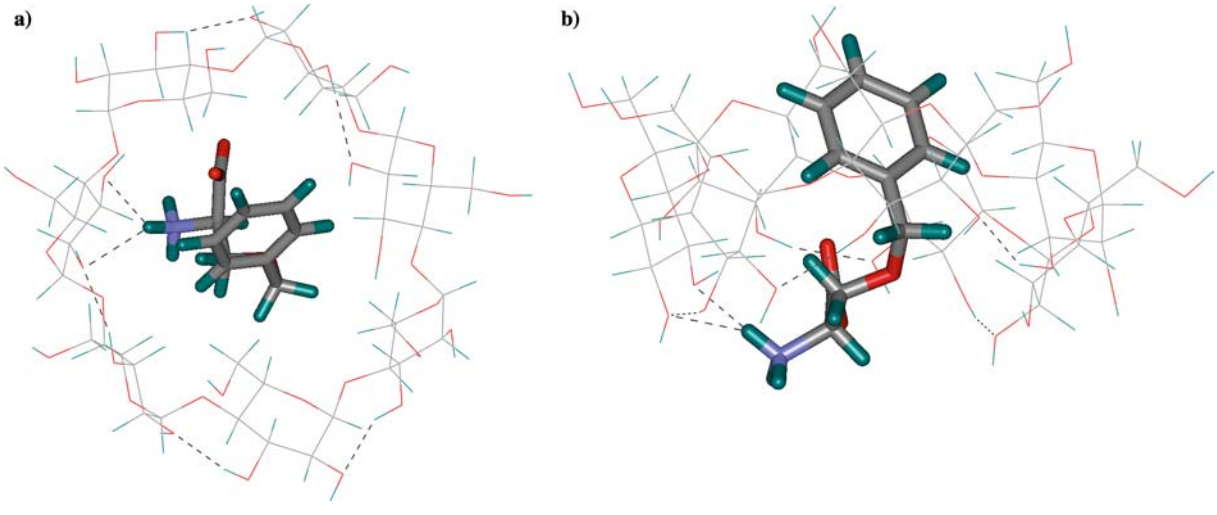

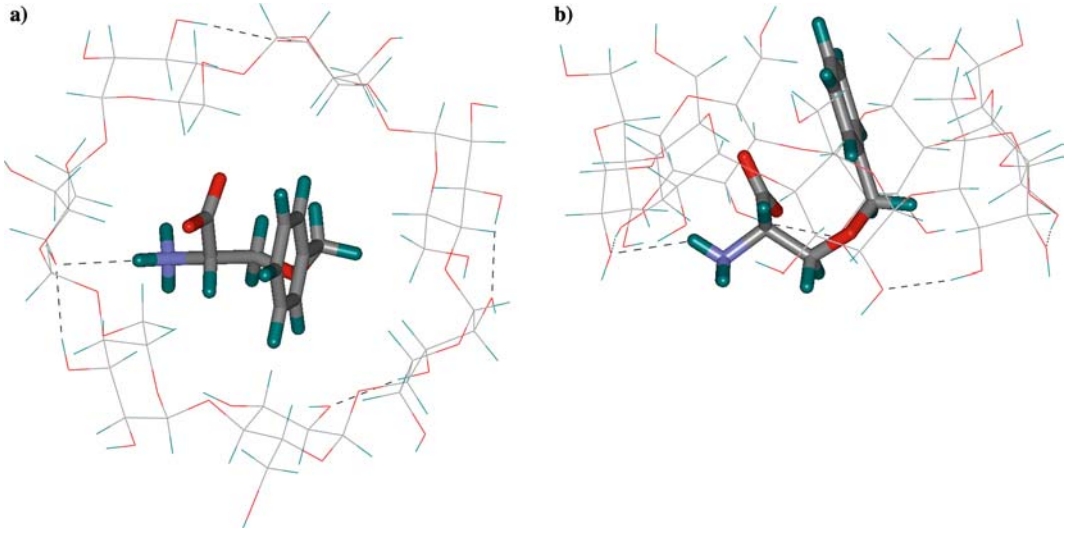

Fig. 5 The favorable structures for the inclusion complexes of L_benzyl_serine with β-CD. β-CD and L_benzyl_serine are drawn in line and stick, respectively. **a** View in the plane normal to the Z-axis. **b** View in the ZX-plane

trostatic effect has a negative effect compared to the van der Waals force in chiral recognition. The compensation between the van der Waals force and the electrostatic interaction leads to an unobservable chiral recognition in real experiment. However, for phenyllactic enantiomeric complexes with the energy differences close in magnitude to that of phenylbutyric, the two main factors contributing to chiral recognition ($\Delta E_{vdw} = -0.368$ kcal mol^{-1}, $\Delta E_{elec} = -0.224$ kcal mol^{-1}) are of the same signs. The two factors can enhance each other in chiral recognition. The cooperativity between the van der Waals force and the electrostatic interaction could possibly lead to a 'hidden mechanism' chiral discrimination. Indeed, an appreciable chiral recognition for phenyllactic has been observed experimentally [3].

Fig. 6 The favorable structures for the inclusion complexes of (R)_phenylbutyric with β-CD. **a** View in the ZX-plane. β-CD and (R)_phenylbutyric are drawn in line and stick, respectively. **b** View in the plane normal to the Z-axis. β-CD is shown in surface and (R)_phenylbutyric in CPK representation

Structural properties responsible for chiral recognition

To elucidate the structural features responsible for the chiral recognition, several typical complex structures were proposed. For example for D/L_benzyl_serine with the favorable complex model A, Figs. 4 and 5 give the corresponding complex structures of D-isomer and L-isomer, respectively. For the structure of D-isomer, there are two hydrogen bonds formed but one for the structure of L-isomer. In the CFF91 force field, the forming and breaking of hydrogen bonds are mainly reflected by a change of electrostatic interaction. Therefore, the difference of hydrogen bonds between the complexes of D_isomer and L_isomer leads to the difference of electrostatic energy between enantiomeric complexes. In addition, the Z-coordinates indicate that the penetration degree of L-isomer is larger than that of D-isomer.

The difference between the enantiomeric complexes is not only reflected by the differences in hydrogen bond and the degree of penetration, but also indicated by the accommodation of phenyl moiety. For (R/S)_phenylbutyric with the favorable complex model A, the main energy difference exists in the van der Waals force term, and the van der Waals interaction of (S)-isomer is stronger than that of (R)-isomer. The structures of the enantiomeric complexes are shown in Figs. 6 and 7, respectively. For (R)-isomer, the phenyl moiety is pre-

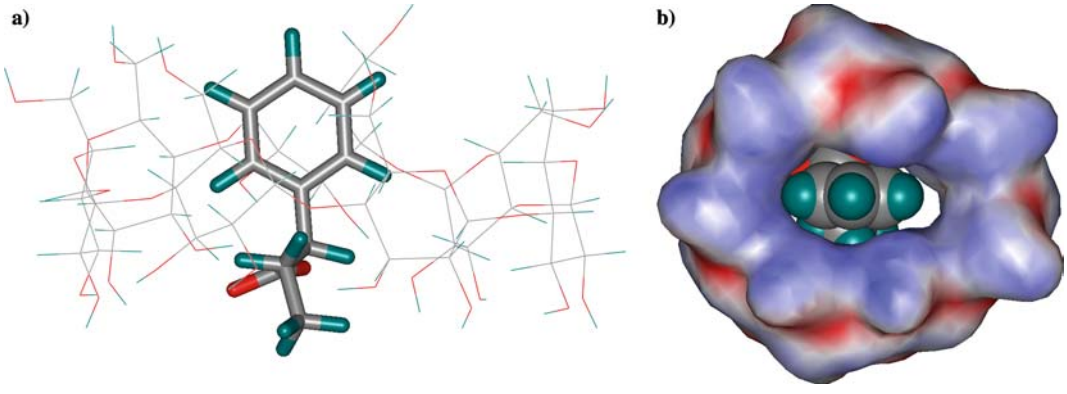

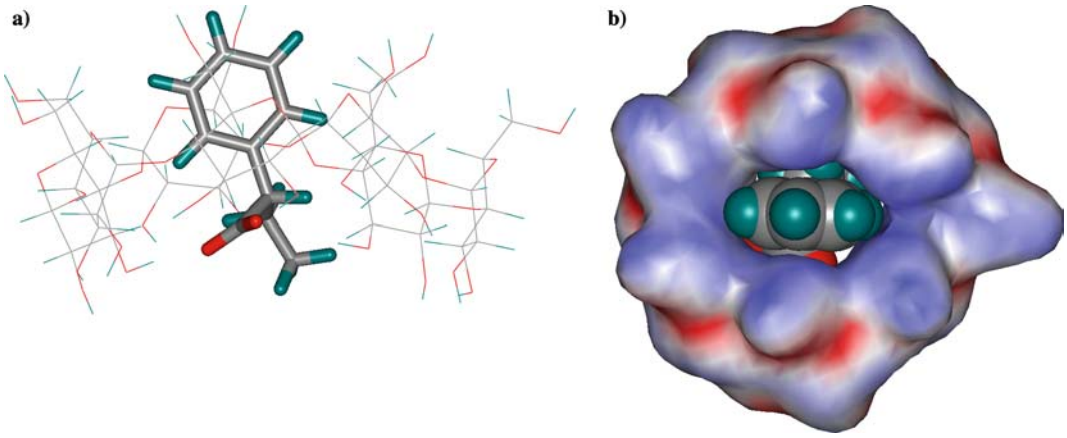

Fig. 7 The favorable structures for the inclusion complexes of (*S*)_phenylbutyric with β-CD. **a** View in the *ZX*-plane. β-CD and (*S*)_phenylbutyric are drawn in line and stick, respectively. **b** View in the plane normal to the *Z*-axis. β-CD is shown in surface and (*S*)_phenylbutyric in CPK representation

ferred to be upright in the cavity (as in Fig. 6a), while the (*S*)-isomer has a tilted position in the cavity (as in Fig. 7a). Moreover, from Figs. 6b and 7b, it can be seen that (*S*)-isomer of phenylbutyric (as in Fig. 7b) contacts more tightly than (*R*)-isomer (as in Fig. 6b) with the cavity. Indeed, the tilted (*S*)-isomer probably leads to closer packing with an increased van der Waals interaction.

Conclusions

The chiral recognition of nine pairs of aromatic chiral compounds was studied using a flexible docking algorithm FDOCK. Two distinct inclusion orientations of the guest molecule were taken into account. The calculated results show that although the preferred orientation is determined, the other one may contribute to the stability constants. Furthermore, the dominant forces holding the host-guest complexes together are the van der Waals forces, and the chiral recognition of the selected enantiomer pairs is the result of the van der Waals force cooperating or compensating with the electrostatic interaction and the hydrophobic effect.

Acknowledgements This study is supported by the Natural Science Foundation of China (No. 20172048) and the Teaching and Research Award Program for Outstanding Young Professors (TRAPOYP) in Higher Education Institute, MOE, P.R.C. The construction and optimization of the structures used in this study by Insight II were completed in the laboratory of UMR 7565 CNRS/UHP, Université H. Poincaré, France.

References

1. Szejtli J (1998) Chem Rev 98:1743–1753
2. Rekharsky MV, Yamamura H, Kawai M, Inoue Y (2001) J Am Chem Soc 123:5360–5361
3. Rekharsky MV, Inoue Y (2000) J Am Chem Soc 122:4418–4435
4. Rekharsky MV, Inoue Y (2002) J Am Chem Soc 124:813–826
5. Alexander JM, Clark JL, Brett TJ, Stezowski JJ (2002) Proc Natl Acad Sci USA 99:5115–5120
6. Lai XH, Ng SC (2004) J Chromatogr A 1031:135–142
7. Lee S, Yi DH, Jung S (2004) B Kor Chem Soc 25:216–220
8. Liu Y, Chen Y, Li L, Li B, Zhang HY (2002) Supramol Chem 14:299–307
9. Lipkowitz KB (1998) Chem Rev 98:1829–1873
10. Sun M, Liu XH, Yan LS, Luo GA (2003) J Mol Model 9:419–422
11. Lipkowitz KB, Coner R, Peterson MA, Morreale A, Shackelford J (1998) J Org Chem 63:732–745
12. Dodziuk H, Ejchart A, Lukin O, Vysotsky MO (1999) J Org Chem 64:1503–1507
13. Lipkowitz KB, Pearl G, Coner B, Peterson MA (1997) J Am Chem Soc 119:600–610
14. Hayes JM, Stein M, Weiser J (2004) J Phys Chem A 108:3572–3580
15. Xia BY, Cai WS, Shao XG, Guo QX, Maigret B, Pan ZX (2001) J Mol Struc (Theochem) 546:33–38
16. Cai WS, Yao XX, Shao XG, Pan ZX (2004) J Incl Phenom Macro (in press)
17. Betzel C, Saenger W, Hingerty BE, Brown GM (1984) J Am Chem Soc 106:7545–7557
18. Cai WS, Shao XG (2002) J Comput Chem 23:427–435
19. Liu DC, Nocedal J (1989) J Math Prog B 45:503–528
20. Maple JR, Dinur U, Hagler AT (1988) Proc Natl Acad Sci USA 85:5350–5354
21. Fraternali F, van Gunsteren WF (1996) J Mol Biol 256:939–948
22. Hasel W, Hendrickson TF, Still WC (1988) Tetrahedron Comput Methodol 1:103–116
23. Liu L, Guo QX (1999) J Phys Chem B 103:3461–3467